UNIL | Université de Lausanne

Unicentre
CH-1015 Lausanne
http://serval.unil.ch

Year : 2011

FDG PET/CT and MR Imaging in Patients with Liver Metastases from Uveal Melanoma: Results from a Pilot Study

ORCURTO Maria Victoria

ORCURTO Maria Victoria, 2011, FDG PET/CT and MR Imaging in Patients with Liver Metastases from Uveal Melanoma: Results from a Pilot Study

Originally published at : Thesis, University of Lausanne

Posted at the University of Lausanne Open Archive.
http://serval.unil.ch

UNIVERSITE DE LAUSANNE - FACULTE DE BIOLOGIE ET DE MEDECINE

Département de Radiologie
Service de Médecine Nucléaire

FDG PET/CT and MR Imaging in Patients with Liver Metastases from Uveal Melanoma: Results from a Pilot Study

THESE

préparée sous la direction du Professeur Angelika Bischof Delaloye
(sous la co-direction du Professeur Serge Leyvraz)
(avec la collaboration du Professeur John Prior)

et présentée à la Faculté de biologie et de médecine de
l'Université de Lausanne pour l'obtention du grade de

DOCTEUR EN MEDECINE

par

Maria Victoria ORCURTO

Médecin diplômée de l'Université de Buenos Aires, Argentine
Originaire de Genève et Fribourg GE/FR, Suisse

Lausanne

2011

Imprimatur

Vu le rapport présenté par le jury d'examen, composé de

Directeur de thèse	Madame le Professeur honoraire **Angelika Bischof Delaloye**
Co-Directeur de thèse	Monsieur le Professeur **Serge Leyvraz**
Expert	Monsieur le Professeur associé **Daniel Hohl**
Directrice de l'Ecole doctorale	Madame le Professeur **Stephanie Clarke**

la Commission MD de l'Ecole doctorale autorise l'impression de la thèse de

Madame Victoria Orcurto

intitulée

FDG PET/CT and MR Imaging in Patients with Liver Metastases from Uveal Melanoma: Results from a Pilot Study

Lausanne, le 6 février 2012

pour Le Doyen
de la Faculté de Biologie et de Médecine

Madame le Professeur Stephanie Clarke
Directrice de l'Ecole doctorale

^{18}F-fluorodeoxyglucose positron emission tomography/computed tomography and magnetic resonance imaging in patients with liver metastases from uveal melanoma: results from a pilot study

Victoria Orcurto[a], Alban Denys[b], Verena Voelter[c], Ann Schalenbourg[d], Pierre Schnyder[b], Leonidas Zografos[d], Serge Leyvraz[c], Angelika Bischof Delaloye[a] and John O. Prior[a]

Purpose ^{18}F-fluorodeoxyglucose (FDG) positron emission tomography/computed tomography (PET/CT) and MRI are used for detecting liver metastases from uveal melanoma. The introduction of new treatment options in clinical trials might benefit from early response assessment. Here, we determine the value of FDG-PET/CT with respect to MRI at diagnosis and its potential for monitoring therapy.

Material and methods Ten patients with biopsy-proven liver metastases of uveal melanoma enrolled in a randomized phase III trial (NCT00110123) underwent both FDG-PET coupled with unenhanced CT and gadolinium-diethylene triamine pentaacetic acid-enhanced liver MRI within 4 weeks. FDG-PET and MRI were evaluated blindly and then compared using the ratio of lesion to normal liver parenchyma PET-derived standardized uptake value (SUV). The influence of lesion size and response to chemotherapy were studied.

Results Overall, 108 liver lesions were seen: 34 (31%) on both modalities (1–18 lesions/patient), four (4%) by PET/CT only, and 70 (65%) by MRI only. SUV correlated with MRI lesion size ($r = 0.81$, $P < 0.0001$). PET/CT detected 26 of 33 (79%) MRI lesions of more than or equal to 1.2 cm, whereas it detected only eight of 71 (11%) lesions of less than 1.2 cm ($P < 0.0001$). MRI lesions without PET correspondence were small (0.6 ± 0.2 vs. 2.1 ± 1.1 cm, $P < 0.0001$). During follow-up (six patients, 30 lesions), the ratio lesion-to-normal-liver SUV diminished in size-stable lesions (1.90 ± 0.64–1.46 ± 0.50, $P < 0.0001$), whereas it increased in enlarging lesions (1.56 ± 0.40–1.99 ± 0.56, $P = 0.032$).

Conclusion MRI outweighs PET/CT for detecting small liver metastases. However, PET/CT detected at least one liver metastasis per patient and changes in FDG uptake not related to size change, suggesting a role in assessing early therapy response. *Melanoma Res* 00:000–000 © 2011 Wolters Kluwer Health | Lippincott Williams & Wilkins.

Introduction

Uveal melanoma is the most common primary intraocular malignancy in Caucasians, representing 70% of all ocular tumors [1]. Median age at presentation is about 60 years and reported annual incidence ranges from 5.3 to 10.9 cases per million in the USA and 2–8 cases per million in Europe [2,3]. Owing to the lack of lymphatics in the eye, metastatic spread of uveal melanoma is exclusively hematogenous, predominantly to the liver ($\geq 95\%$ of metastatic patients) [4]. Approximately 1% of patients have demonstrable liver metastases at presentation, and up to 50% will ultimately develop hepatic metastases within 10–15 years, suggesting the presence of subclinical disease at the time of initial diagnosis [1]. The mechanisms for this liver tropism is not yet understood [4]. Other less common sites of metastasis are lungs, bones, skin, lymph nodes, pancreas, heart, spleen,

adrenal glands, gastrointestinal tract, kidneys, ovaries, and thyroid. Several clinical, histopathological, and cytogenetic characteristics are associated with poor prognosis including chromosomal abnormalities, the most important of which are monosomy 3, isochromosome 6p, trisomy 8, and isochromosome 8q [5].

Currently, there are no effective treatments to prevent, delay, or treat liver metastases of uveal melanoma, and the median survival after diagnosis of liver metastasis is 2–7 months in historical series [6]. Several regional therapies are clinically used or under investigation in clinical trials to control liver progression, such as hepatic arterial chemotherapy, chemoembolization [6], radioembolization [7], thermoablation [8], or targeted therapies showing potential benefit on overall survival or response rate, even without objective tumor response [4,9]. For

instance, using intra-arterial hepatic fotemustine chemotherapy, median survival of up to 15 months has been observed in association with a 36% response rate and 33% survival rate at 2 years [10].

Positron emission tomography (PET) with ^{18}F-fluorodeoxyglucose (FDG) is a sensitive and an accurate method for the detection of metastases from cutaneous melanoma. Of limited value for the diagnosis of ocular melanoma, it was found to be sensitive for the detection of hepatic and extrahepatic metastases [11–14]. Servois et al. [15] compared the performance of FDG-PET and MRI for staging liver metastasis and concluded that MRI was superior to FDG-PET, but the respective value of FDG-PET and MRI have not been fully assessed in intrapatient comparison for the diagnosis and monitoring of liver metastasis from uveal melanoma [12]. Tumor uptake of FDG is highly reproducible and decrease is known to occur before change in size [16]. Whether this remains true for liver metastases from uveal melanoma is not known.

Early diagnosis of liver metastasis may be important for therapeutic management [17]. Furthermore, early response assessment may benefit the introduction of new treatment options as key oncogenic processes leading to uveal melanoma have been recently identified [18]. Our purpose was to determine the respective value of FDG-PET and MRI in patients with liver metastases of uveal melanoma.

Methods
Patient selection
From 2004 to 2008, 10 patients with known uveal melanoma and at least one histologically-proven liver metastasis were enrolled in a randomized phase III multicentric trial from the Uveal Melanoma Group of the European Organization for Research and Treatment of Cancer (EORTC) comparing the effect on overall survival of hepatic intra-arterial with systemic intravenous administration of fotemustine in patients with liver metastases from uveal melanoma (EORTC-18021, NCT00110123). This trial initiated after a phase II trial at our center showed evidence for improved survival after intra-arterial hepatic fotemustine chemotherapy [19]. The eligibility criteria were age of more than or equal to 18 years, surgically incurable or unresectable disease, and no extrahepatic metastases; whereas the exclusion criteria were previous chemotherapy or radiotherapy, abnormal hematopoiesis, abnormal kidney or liver function, uncontrolled angina pectoris, myocardial infarction for less than 6 months, intracranial hypertension, other severe cardiac disease, and other malignancy for less than 5 years. Patients not having recovered from earlier major surgery or with World Health Organization performance status not more than 2 were also excluded. The protocol was approved by the local ethics committee and the Swiss regulatory authorities, and patients signed informed consent forms before inclusion.

At our center, this protocol included an imaging study comparing MRI and FDG-PET that is presented here. Ten patients (six women, four men; 20–74 years at diagnosis) were studied by MRI and PET/CT within 4 weeks (range, 0–25 days). Of them, six patients were studied at baseline and four early during chemoinduction (after 3–4 cycles of fotemustine). During follow-up, a subgroup of six patients repeated both PET/CT and MRI studies within 4 weeks after a variable time on therapy (7–28 weeks).

Magnetic resonance imaging
Abdominal MRI images were acquired on a 1.5 T ($n = 5$) and 3 T ($n = 5$) scanner (Symphony, Siemens Healthcare, Erlangen, Germany) with a maximum gradient strength of 40 mT/m using a four-channel phased-array body coil with a 35×25-cm field of view, and bandwidth was 1346 Hz. The liver protocol encompassed a breath-hold, T2-weighted transverse half-Fourier single-shot turbo spin echo sequence (repetition time/echo time = 1100 ms/59 ms, echo train length = 256, matrix = 256×148, slab thickness/gap = 3 mm/0.9 mm), a T1-weighted transverse spoiled gradient-echo sequence (in-phase: 167/4.8; out-phase: 167/2.4, 256×134, 6/2; flip angle, 70°), a respiratory-triggered T2-weighted transverse fat-suppressed fast spin-echo sequence (6361.3/121, echo train length = 23, 512×188, 6/1.8) and a breath-hold T1-weighted transverse fat-suppressed gradient-echo sequences (3.7/1.6, 256×192, 4/0.8, flip angle 12°, number of excitations = 1). The latter was performed before and after intravenous gadolinium-diethylene triamine penta-acetic acid (Gd-DTPA) injection (arterial, portovenous, and equilibrium phases; 0.1 mmol/kg Omniscan; GE Healthcare, Milwaukee, Wisconsin, USA). Liver lesions were considered suspicious for metastases when presenting a short T1 pattern (high signal intensity) without injection, an arterial Gd-DPTA enhancement and a short T2 pattern (low signal intensity) compared with adjacent normal liver; solitary lesions with short T1 pattern and a long T2 pattern were also considered as suspicious [20].

[18]F-fluorodeoxyglucose positron emission tomography/computed tomography
Whole-body PET/CT (Discovery LS scanner, GE Healthcare) was acquired 67 ± 15 min after intravenous bolus injection of FDG (5 MBq/kg) using standard PET/CT acquisition protocols. Patients had been fasting for more than or equal to 6 h and blood glucose at injection was less than 8.3 mmol/l. Attenuation correction was performed using an unenhanced CT (140 keV, 80 mA, 0.8 s per rotation, table speed of 15 mm/rotation, slice thickness of 5 mm). Liver lesions were considered suspicious for metastases when FDG uptake was focally increased compared with surrounding liver on at least two consecutive 5-mm slices.

Image analysis
An experienced radiologist evaluated the MR images and an experienced nuclear medicine specialist evaluated the

PET images. Each reader was blinded to the results of the other modality. For MR, hepatic lesions were numbered, evaluated and their largest diameter measured. For each suspicious liver lesion, maximal standardized uptake value (SUV) corrected for body weight was obtained. To facilitate result comparison with other PET centers, we expressed the lesion SUV normalized to normal liver parenchyma SUV ('lesion-to-liver SUV ratio') by dividing the lesion SUV by liver SUV averaged in a volume of more than or equal to $27\,cm^3$ in a region with uniform activity on PET distant from areas with abnormally increased or decreased FDG uptake. In a second reading, MRI and PET images were subsequently compared with each other to classify each lesion as being detected by both (MR + PET) or a single modality (MRI or PET). The intrinsically low resolution of PET scanners and the three-dimensional voxel sampling contribute to the 'partial volume effect,' which significantly diminishes the apparent SUV in lesions smaller than twice the PET scanner resolution [21]. Therefore, referring to the known spatial resolution of our scanner of about 6 mm [22], a subgroup analysis was performed according to lesion size of less than 1.2 and more than or equal to 1.2 cm diameter.

Statistical analysis
Results are presented as mean ± standard deviation, if not specified otherwise. Group comparisons were made using unpaired Student's *t*-tests for continuous variables and the χ^2-test for categorical variables. Lesion changes from baseline to follow-up used paired Student's *t*-test, and associations were sought using Pearson's correlations. Significance was considered for *P* values of less than 0.05.

Results
Patient characteristics
Table 1 summarizes patient and tumor characteristics: no patient presented with a T1 tumor, one with a T2 (10%), seven with a T3 (70%), and two with a T4 (20%) tumor, according to the Tumor Node Metastasis-American Joint Cancer Committee classification [23] and three patients already had liver metastasis at primary diagnosis (M1). The median interval between the primary diagnosis of uveal melanoma and the detection of hepatic metastasis was 3.0 years (range: 0–10 years). No significant correlation was found between SUV on one hand and the total number of lesions, tumor height, largest basal diameter or Tumor Node Metastasis-American Joint Cancer Committee classification on the other hand (all *P* > 0.44).

Lesion detection according to imaging modality
Overall, 108 suspicious liver lesions were seen by MRI or PET (Table 2). Of these lesions, 34 (31%) were seen on both PET and MRI, four (4%) only on PET, and 70 (65%) only on MRI, among which 41 were seen in one patient

(Figs. 1 and 2). On a per-patient basis, at least one liver metastasis (range 1–18) was detected with PET in all patients.

Influence of lesion size
As expected, MRI more often detected small-sized lesions, whereas most lesions of more than or equal to 1.2 cm could be seen on both modalities. Twenty six of 33 (79%) lesions of more than or equal to 1.2 cm on MRI were visualized by PET, whereas this was the case for only eight of 71 (11%) lesions of less than 1.2 cm (*P* < 0.0001). Moreover, lesions of less than 1.2 cm had significantly lower SUV than more than or equal to 1.2 cm lesions (3.1 ± 0.5 vs. 4.7 ± 1.8 g/ml, *P* < 0.0001; Fig. 3).

^{18}F-fluorodeoxyglucose positron emission tomography standardized uptake value
For lesions detected by both modalities, there was a strong correlation between SUV [SUV (g/ml) = 2.9 + 1.06 MRI size (cm), *r* = 0.76, *P* < 0.0001], as well as between the lesion-to-liver SUV ratio (*r* = 0.81, *P* < 0.0001) and MRI lesion size (Fig. 4). Of note, there were eight subcentimetric lesions detected by PET with SUV significantly increased above liver background (3.8 ± 0.5 vs. 3.0 ± 0.4 g/ml, *P* < 0.0001; Fig. 4). PET lesions with no corresponding MRI lesion presented significantly elevated SUV compared with liver background (4.0 ± 0.5 vs. 3.0 ± 0.4 g/ml, *P* < 0.0001; Fig. 5). MRI lesions without corresponding PET lesion were significantly smaller (0.6 ± 0.2 vs. 2.1 ± 1.1 cm, *P* < 0.0001; Fig. 6).

Lesion monitoring during chemotherapy
Median time between baseline and follow-up imaging was 2.6 months (range, 1.5–6.5 months) in the group of six patients imaged twice (*n* = 30 lesions in total). As any change in lesion size can influence the measured SUV, a subgroup analysis was performed for lesions detected on both MRI and PET/CT according to change in lesion size (no significant change in size vs. increase in MR-measured largest lesion diameter). The mean SUV of liver did not change significantly from baseline to follow-up (2.93 ± 0.46 vs. 2.81 ± 0.25, *P* = 0.7). In five patients, lesion size (26 lesions) did not change significantly, whereas one patient (four lesions) progressed rapidly after 3.9 months, as illustrated in Fig. 7. In stable lesions (*n* = 26), lesion-to-liver SUV ratio significantly decreased (from 1.90 ± 0.64 to 1.46 ± 0.50, *P* < 0.0001), whereas in growing lesions (*n* = 4) lesion-to-liver SUV ratio increased (1.56 ± 0.40–1.99 ± 0.56, *P* = 0.032).

Discussion
Our study on 10 patients with hepatic metastases from uveal melanoma, adding together over 100 liver lesions observed on MRI and PET, only 31% of the secondary lesions were seen on both modalities; whereas most lesions inferior to 1 cm were missed on FDG-PET. Our

Table 1 Patients and tumors characteristics

Patient number	Sex	Age (years)[a]	Eye side	Tumor size (mm)[b]		TNM-AJCC (stage)	Primary tumor therapy
				Height	Largest basal diameter		
1	Man	73	Right	2.9	13.1	T4N0M1 (IV)	Proton therapy
2	Woman	69	Left	3.1	14.2	T2N0M0 (II)	Proton therapy
3	Woman	30	Left	5.8	16.3	T3N0M0 (III)	Proton therapy
4	Man	39	Left	5.8	23.5	T3N0M0 (III)	Proton therapy
5	Woman	20	Left	6.8	15.6	T3N0M0 (III)	Proton therapy
6	Man	74	Right	7.0	7.0	T3N0M0 (III)	Enucleation
7	Man	56	Left	9.0	19.0	T3N0M0 (III)	Proton therapy
8	Woman	72	Right	11.4	19.1	T3N0M1 (IV)	Proton therapy
9	Woman	57	Right	12.7	23.3	T3N0M1 (IV)	Proton therapy
10	Woman	71	Left	16.0	15.0	T4N0M0 (III)	Enucleation

AJCC, American Joint Cancer Committee Classification; TNM, tumor node metastasis.
[a]At diagnosis of primary tumor.
[b]Tumor size of tumors treated by proton therapy cannot be compared with tumor size of enucleation, as the height and largest basal diameter were measured by ultrasound and preoperative transillumination respectively in the former and derived from the histopathology report in the latter.

**Table 2 Positron emission tomography and MRI imaging findings**

Patient	Number of MRI lesions	Number of PET lesions	Number of lesions seen both on PET and MRI (%)	Number of small-sized lesions [mean (range), cm][a]
1	2	1	1 (50)	2 [0.9 (0.8–1.0)]
2	4	3[b]	2 (50)	3 [0.8 (0.5–1.0)]
3	2	2	2 (100)	0 (–)
4	41	18	18 (44)	20 [0.7 (0.3–1.1)]
5	2	2[b]	1 (50)	2 [0.9 (0.8–0.9)]
6	26	4	4 (15)	21 [0.5 (0.5–1.1)]
7	3	3	3 (100)	2 [0.8 (0.8–0.8)]
8	4	2[b]	1 (25)	3 [0.4 (0.4–0.4)]
9	8	2[b]	1 (13)	7 [0.5 (0.3–0.8)]
10	12	1	1 (8)	11 [0.5 (0.4–1.0)]
Total	104	38	34 (33)	71 [(0.3–1.1)]

[a]Defined as size < 1.2 cm, which corresponds to twice the PET/CT spatial resolution [22].
[b]One PET lesion not visible on MRI.
CT, computed tomography; PET, positron emission tomography.
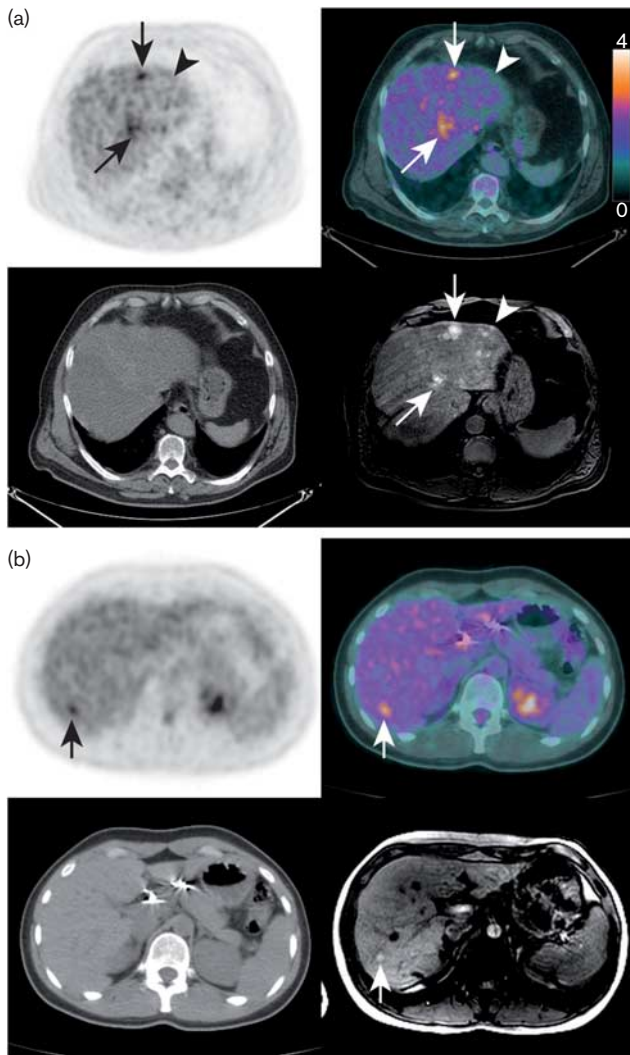
Fig. 1
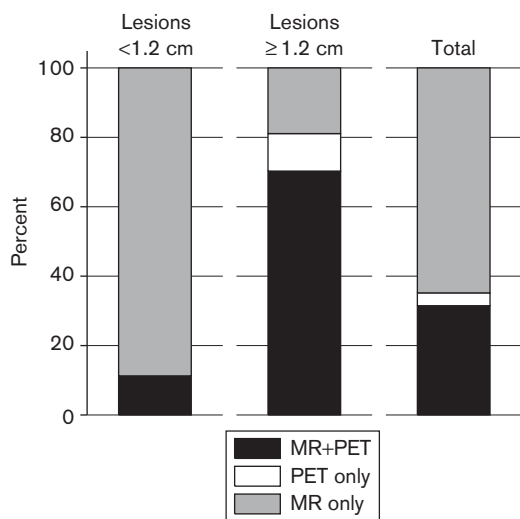
Lesion detectability according to imaging modality and lesion size. The vast majority of small lesions of less than 1.2 cm, were only visualized by MRI, whereas the larger lesions of more than or equal to 1.2 cm were mostly visualized by both, MRI and positron emission tomography (PET). A few lesions were only detected on PET.

data therefore confirm the findings of Servois *et al.* [15], showing that MRI outweighs PET/CT performance for detecting small-sized liver metastases. In consequence, MRI appears to be the preferred method for evaluating number and topography of liver metastases potentially treatable by local therapy such as surgery, radiofrequency ablation, chemoembolization, or radioembolization. The partial volume effect and artifacts from respiratory movements during acquisition prevented detection of most small-sized metastases. Nevertheless, a few infra-centimetric lesions (11%) expressed an increased FDG uptake. When considering larger sizes (≥ 1.2 cm), 79% of the lesions were visualized by both modalities. On a per-patient basis, FDG-PET proved to be a sensitive investigation, as it detected the presence of at least one liver metastasis in every patient of our population. This allowed changes to be observed in the metabolic activity of lesions between baseline and follow-up examinations, even in the absence of a change in lesion size on MRI.

Our study compared MRI with FDG-PET in the same patient. Francken *et al.* [13] evaluated the detectability of liver metastasis by PET in a cohort of 22 patients, which showed a high sensitivity (10/10), a moderate specificity (67%), as well as positive and negative predictive
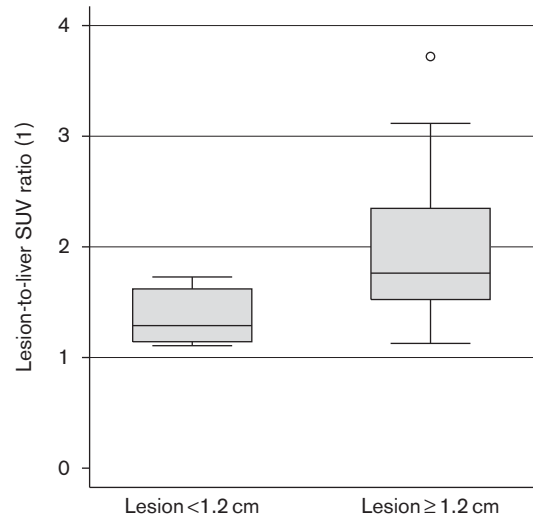
Fig. 2

Fig. 3

Boxplot of the lesion to liver standardized uptake value (SUV) ratio, which is significantly lower for smaller lesions (<1.2 cm) compared with larger lesions (≥ 1.2 cm; *P*<0.0001).

Fig. 4

Plot of the standardized uptake value (SUV) of the lesion-to-liver SUV ratio versus MRI lesion size for lesions visible on both modalities. There was a significant correlation between lesion-to-liver SUV ratio and lesion size, even above twice the positron emission tomography/computed tomography (PET/CT) resolution ($y = 0.79 + 0.44x$, $r = 0.81$, *P*<0.0001). Note that eight lesions smaller than twice the PET/CT resolution (1.2 cm, dashed line) were also detected on PET/CT.

^{18}F-fluorodeoxyglucose positron emission tomography (PET), PET/computed tomography (CT) fusion, unenhanced CT and MRI transaxial images of two patients: (a) A 78-year-old man with several lesions detected on both PET and MRI (arrows) and several smaller lesions detected on MRI only (arrowhead) showing hypersignal on T1-weighted fat-suppressed gradient-echo [repetition time (TR), 3.7 ms; echo time (TE), 1.6 ms; flip angle, 12°)]; (b) a 33-year-old woman with one 8-mm lesion detected on both PET and MRI (arrow) showing an hypersignal on unenhanced T1-weighted spoiled gradient-echo in-phase (TR, 167 ms; TE, 4.8 ms; flip angle, 70°) and out-phase (TR, 167 ms; TE, 2.4 ms; flip angle, 70°).
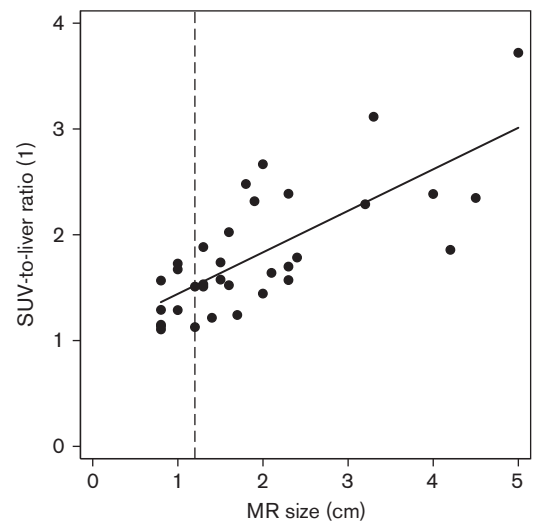
values of 88 and 100%, respectively. They concluded that FDG-PET was particularly useful in the detection of isolated, potentially resectable liver metastases. The present study does not confirm these initial results, as many more liver lesions were detected by MRI alone (PET detection rate 33%), whereas only four lesions were shown by FDG-PET and not by MRI. These lesions were of limited extension (< 3 pixels or < 1.2 cm) and of unknown origin (no histopathological proof was available,
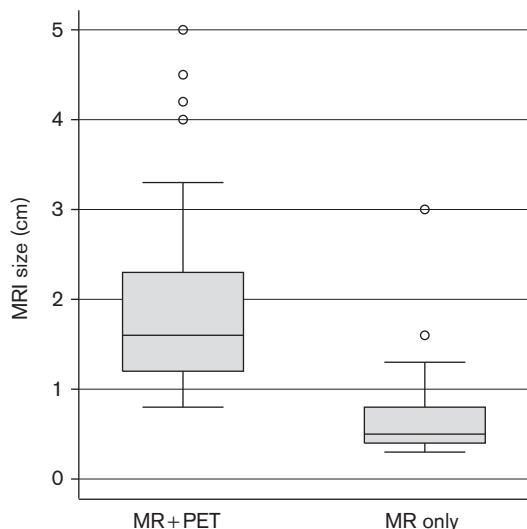
as it was deemed not clinically necessary for patient management). Thus, an artifact at PET or a false-negative MRI cannot be excluded. MRI should therefore be considered the method of choice for detecting liver metastases of uveal melanoma and characterizing liver

Fig. 5
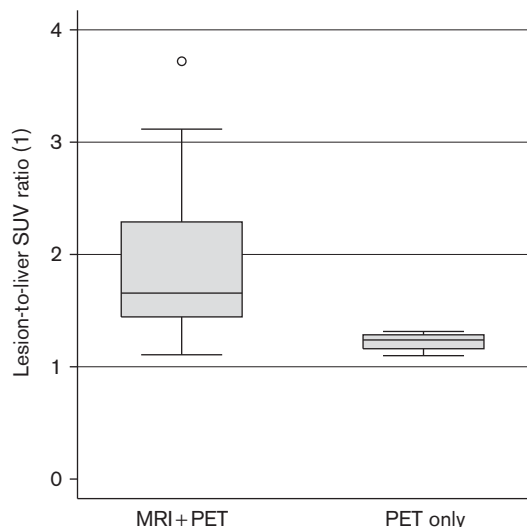
Boxplot of the ratio of lesion standardized uptake value (SUV) to liver parenchyma SUV according to visualization by MRI + positron emission tomography (PET) or PET alone. The lesion-to-liver SUV ratio of lesions visible by both modalities (MRI + PET) was significantly higher than unity ($P < 0.0001$).

Fig. 7

Variation in lesion-to-liver standardized uptake value (SUV) ratio between baseline [positron emission tomography (PET 1)] and follow-up study (PET 2) according to change in lesion size as measured by MRI, no change vs. increase in size for patients with lesions visible on both ^{18}F-fluorodeoxyglucose-PET and MRI at baseline (six patients, 30 lesions in total).
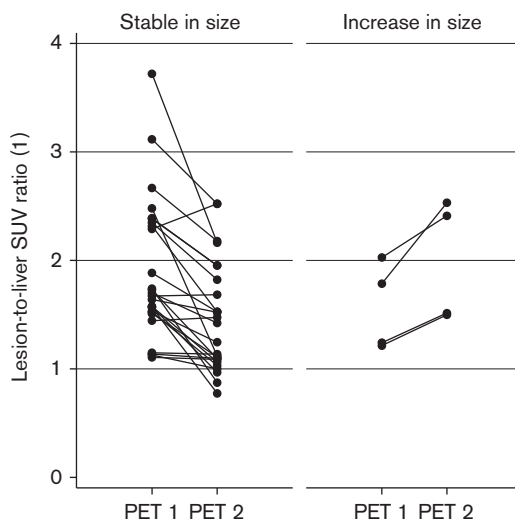
Fig. 6

Boxplot of the lesion size according to visualization by MRI + positron emission tomography (PET) or MRI alone. The diameter of lesions visible by both modalities (MRI + PET) was significantly larger than lesions visible only by MRI ($P < 0.0001$).

involvement potentially amenable to local therapy. Our findings are in line with recent results by Strobel et al. [24] showing limited value of FDG-PET in the detection of liver metastasis from uveal melanoma compared with cutaneous melanoma, with a PET detection rate of only 41% (11/27 metastases).

Importantly, serial PET was able to detect short-term changes in the metabolic activity of lesions despite the absence of size change. This has significant implications for the early assessment of therapy response and FDG-PET assessment of metastases has been proposed both as a surrogate marker of treatment response and as a prognostic factor for overall survival [25]. Identifying responders and nonresponders might improve clinical management in term of side effects and costs [26].

Baseline SUV was found to be proportional to MRI size, including lesions with dimensions well above those where the partial volume effect is no longer expected to play a role. In fact, larger SUV values reflect an increased rate of glycolysis and have been strongly associated with increased tumor aggressiveness and poorer outcome in a number of cancers such as lung cancer, esophageal cancer, or thyroid carcinoma [25,27]. Whether baseline SUV remains an independent prognostic marker in addition to the largest dimension of liver metastases needs to be verified in an outcome study following published guidelines [28].

Obviously, the small size and heterogeneity of our patient population does not allow to evaluate the effect of treatment response according to the administration route or chemotherapeutic regimen, which is the aim of the multicentric EORTC-18021 study, but with over 100 lesions, comparisons between MRI and PET can be considered valid. Four patients had already started chemotherapy at first PET, which may diminish PET

sensitivity. Another potential limitation is that the diagnosis of metastatic liver lesions was based on their characteristic MRI appearance, as it is obviously not possible to biopsy all liver lesions. Thus, false-positive lesions at MRI cannot be excluded, but the combination of T1 weighting and T2 weighting, and behavior after gadolinium-diethylene triamine pentaacetic acid injection increase specificity. For a few patients, a dual-phase PET/CT was performed with a late phase taken after 90 min or more, which seemed to improve lesion detectability by increasing lesion SUV and lesion-to-liver SUV ratio (data not shown); delayed FDG-PET acquisition might therefore improve the detection of small metastases, as has been demonstrated for several other tumors as well as primary uveal melanomas [14]. Diffusion-weighted MRI was not performed in this study, but might be valuable in assessing response to therapy, if preliminary results showing treatment related changes in the apparent diffusion coefficient are confirmed [29]. Finally, our pilot study was not designed to determine the predictive value of PET or MRI for therapy response.

Conclusion
In this pilot study, MRI outweighs FDG-PET performance for detecting small-sized liver metastases and is therefore the preferred method for diagnosing the number and the topography of liver metastases. However, PET/CT showed a decreased FDG uptake in the absence of MRI change under chemotherapy and an increased FDG uptake in lesions increasing in size at follow-up suggesting a possible role for monitoring treatment response. This underlines the need of determining the value of FDG-PET/CT in predicting long-term response to therapy in patients with liver metastases from uveal melanoma in a prospective study.

References
1 Mudhar HS, Parsons MA, Sisley K, Rundle P, Singh A, Rennie IG. A critical appraisal of the prognostic and predictive factors for uveal malignant melanoma. *Histopathology* 2004; **45**:1–12.
2 Singh AD, Topham A. Incidence of uveal melanoma in the United States: 1973–1997. *Ophthalmology* 2003; **110**:956–961.
3 Virgili G, Gatta G, Ciccolallo L, Capocaccia R, Biggeri A, Crocetti E, *et al.* Incidence of uveal melanoma in Europe. *Ophthalmology* 2007; **114**:2309–2315.
4 Bakalian S, Marshall JC, Logan P, Faingold D, Maloney S, Di Cesare S, *et al.* Molecular pathways mediating liver metastasis in patients with uveal melanoma. *Clin Cancer Res* 2008; **14**:951–956.
5 Damato B, Dopierala J, Klaasen A, Van Dijk M, Sibbring J, Coupland SE. Multiplex ligation-dependent probe amplification of uveal melanoma: correlation with metastatic death. *Invest Ophthalmol Vis Sci* 2009; **50**:3048–3055.
6 Feldman ED, Pingpank JF, Alexander HR Jr. Regional treatment options for patients with ocular melanoma metastatic to the liver. *Ann Surg Oncol* 2004; **11**:290–297.
7 Kennedy AS, Nutting C, Jakobs T, Cianni R, Notarianni E, Ofer A, *et al.* A first report of radioembolization for hepatic metastases from ocular melanoma. *Cancer Invest* 2009; **27**:682–690.
8 Kuvshinoff B, Fong Y. Surgical therapy of liver metastases. *Semin Oncol* 2007; **34**:177–185.
9 Triozzi PL, Eng C, Singh AD. Targeted therapy for uveal melanoma. *Cancer Treat Rev* 2008; **34**:247–258.
10 Peters S, Voelter V, Zografos L, Pampallona S, Popescu R, Gillet M, *et al.* Intra-arterial hepatic fotemustine for the treatment of liver metastases from uveal melanoma: experience in 101 patients. *Ann Oncol* 2006; **17**:578–583.
11 Reddy S, Kurli M, Tena LB, Finger PT. PET/CT imaging: detection of choroidal melanoma. *Br J Ophthalmol* 2005; **89**:1265–1269.
12 Kurli M, Reddy S, Tena LB, Pavlick AC, Finger PT. Whole body positron emission tomography/computed tomography staging of metastatic choroidal melanoma. *Am J Ophthalmol* 2005; **140**:193–199.
13 Francken AB, Fulham MJ, Millward MJ, Thompson JF. Detection of metastatic disease in patients with uveal melanoma using positron emission tomography. *Eur J Surg Oncol* 2006; **32**:780–784.
14 Beyer T, Pietrzyk U, Knoess C, Vollmar S, Wienhard K, Kracht L, *et al.* Multi-modality imaging of uveal melanomas using combined PET/CT, high-resolution PET and MR imaging. *Nuklearmedizin* 2008; **47**:73–79.
15 Servois V, Mariani P, Malhaire C, Petras S, Piperno-Neumann S, Plancher C, *et al.* Preoperative staging of liver metastases from uveal melanoma by magnetic resonance imaging (MRI) and fluorodeoxyglucose-positron emission tomography (FDG-PET). *Eur J Surg Oncol* 2010; **36**:189–194.
16 Weber WA, Ziegler SI, Thodtmann R, Hanauske AR, Schwaiger M. Reproducibility of metabolic measurements in malignant tumors using FDG PET. *J Nucl Med* 1999; **40**:1771–1777.
17 Aoyama T, Mastrangelo MJ, Berd D, Nathan FE, Shields CL, Shields JA, *et al.* Protracted survival after resection of metastatic uveal melanoma. *Cancer* 2000; **89**:1561–1568.
18 Van Raamsdonk CD, Griewank KG, Crosby MB, Garrido MC, Vemula S, Wiesner T, *et al.* Mutations in GNA11 in uveal melanoma. *N Engl J Med* 2010; **363**:2191–2199.
19 Leyvraz S, Spataro V, Bauer J, Pampallona S, Salmon R, Dorval T, *et al.* Treatment of ocular melanoma metastatic to the liver by hepatic arterial chemotherapy. *J Clin Oncol* 1997; **15**:2589–2595.
20 Maeda T, Tateishi U, Suzuki S, Arai Y, Kim EE, Sugimura K. Magnetic resonance screening trial for hepatic metastasis in patients with locally controlled choroidal melanoma. *Jpn J Clin Oncol* 2007; **37**:282–286.
21 Soret M, Bacharach SL, Buvat I. Partial-volume effect in PET tumor imaging. *J Nucl Med* 2007; **48**:932–945.
22 Bolard G, Prior JO, Modolo L, Delaloye AB, Kosinski M, Wastiel C, *et al.* Performance comparison of two commercial BGO-based PET/CT scanners using NEMA NU 2-2001. *Med Phys* 2007; **34**:2708–2717.
23 American Joint Committee on Cancer. *Malignant melanoma of the uvea AJCC Cancer Staging Manual.* 6th edn. New York, NY: Springer. 2002; pp. 365–370.
24 Strobel K, Bode B, Dummer R, Veit-Haibach P, Fischer D, Imhof L, *et al.* Limited value of 18F-FDG PET/CT and S-100B tumour marker in the detection of liver metastases from uveal melanoma compared to liver metastases from cutaneous melanoma. *Eur J Nucl Med Mol Imaging* 2009; **36**:1774–1782.
25 Larson SM, Schwartz LH. 18F-FDG PET as a candidate for 'qualified biomarker': functional assessment of treatment response in oncology. *J Nucl Med* 2006; **47**:901–903.
26 Prior JO, Montemurro M, Orcurto MV, Michielin O, Luthi F, Benhattar J, *et al.* Early prediction of response to sunitinib after imatinib failure by 18F-fluorodeoxyglucose positron emission tomography in patients with gastrointestinal stromal tumor. *J Clin Oncol* 2009; **27**:439–445.
27 Downey RJ, Akhurst T, Gonen M, Vincent A, Bains MS, Larson S, *et al.* Preoperative F-18 fluorodeoxyglucose-positron emission tomography maximal standardized uptake value predicts survival after lung cancer resection. *J Clin Oncol* 2004; **22**:3255–3260.
28 Shankar LK, Hoffman JM, Bacharach S, Graham MM, Karp J, Lammertsma AA, *et al.* Consensus recommendations for the use of 18F-FDG PET as an indicator of therapeutic response in patients in National Cancer Institute trials. *J Nucl Med* 2006; **47**:1059–1066.
29 Buijs M, Vossen JA, Hong K, Georgiades CS, Geschwind JF, Kamel IR. Chemoembolization of hepatic metastases from ocular melanoma: assessment of response with contrast-enhanced and diffusion-weighted MRI. *AJR Am J Roentgenol* 2008; **191**:285–289.